HHS Public Access

Author manuscript

Biomaterials. Author manuscript; available in PMC 2015 September 10.

Published in final edited form as:

Biomaterials. 2015 August ; 59: 160–171. doi:10.1016/j.biomaterials.2015.04.025.

Inhibition of MAP kinase/NF-kB mediated signaling and attenuation of lipopolysaccharide induced severe sepsis by cerium oxide nanoparticles

Vellaisamy Selvaraj[a], **Niraj Nepal**[a], **Steven Rogers**[a], **Nandini D.P.K. Manne**[a], **Ravikumar Arvapalli**[a], **Kevin M. Rice**[a], **Shinichi Asano**[a], **Erin Fankhanel**[a], **Jane J. Ma**[e], **Tolou Shokuhfar**[f], **Mani Maheshwari**[a], and **Eric R. Blough**[a,b,c,d,*]

[a]Center for Diagnostic Nanosystems, Marshall University, Huntington, WV, USA

[b]Department of Pharmacology, Physiology and Toxicology, Joan C. Edwards School of Medicine, Marshall University, Huntington, WV, USA

[c]Department of Cardiology, Joan C. Edwards School of Medicine, Marshall University, Huntington, WV, USA

[d]Department of Pharmaceutical Sciences and Research, School of Pharmacy, Marshall University, Huntington, WV, USA

[e]Health Effects Laboratory Division, NIOSH, Morgantown, WV, USA

[f]Department of Mechanical Engineering and Engineering Mechanics, Michigan Technological University, Houghton, MI, USA

Abstract

Sepsis is a life threatening disease that is associated with high mortality. Existing treatments have failed to improve survivability in septic patients. The purpose of this present study is to evaluate whether cerium oxide nanoparticles (CeO_2NPs) can prevent lipopolysaccharide (LPS) induced severe sepsis mortality by preventing hepatic dysfunction in male Sprague Dawley rats. Administration of a single dose (0.5 mg/kg) of CeO_2NPs intravenously to septic rats significantly improved survival rates and functioned to restore body temperature, respiratory rate and blood pressure towards baseline. Treatment-induced increases in animal survivability were associated with decreased hepatic damage along with reductions in serum cytokines/chemokines, and diminished inflammatory related signaling. Kupffer cells and macrophage cells exposed to CeO_2NPs exhibited decreases in LPS-induced cytokine release (TNF-α, IL-1β, IL-6, HMGB1) which were associated with diminished cellular ROS, reduced levels of nitric oxide synthase (iNOS), cyclooxygenase 2 (COX-2), and decreased nuclear factor-kappa light chain enhancer of activated B cells (NF-kB) transcriptional activity. The findings of this study indicate that CeO_2NPs may be useful as a therapeutic agent for sepsis.

*Corresponding author. Center for Diagnostic Nanosystems, Room 241N, Robert C. Byrd Biotechnology Science Center, 1700 3rd Ave., Marshall University, Huntington, WV 25755-1090, USA. Tel.: +1 304 696 2708; fax: +1 304 696 3766. blough@marshall.edu (E.R. Blough).

Conflict of interest: The authors declare no conflict of interest.

Keywords

Cerium oxide nanoparticles; Lipopolysaccharide; Sepsis; Cytokines; Macrophage

1. Introduction

Severe sepsis is associated with a systemic inflammatory response syndrome (SIRS) that is characterized by widespread elevations in reactive oxygen species (ROS) and increased levels of circulating tumor necrosis factor-α (TNF-α) and interleukin 6 (IL-6). The development of SIRS is a primary cause of multiple-organ dysfunction syndrome (MODS) and death in septic patients [1,2]. Although the SIRS response can be elicited by mycobacteria, parasites, fungus, and viruses it is thought that exposure to gram negative bacteria and lipopolysaccharide (LPS) is the predominant cause [3,4]. Amongst the different organ systems affected by sepsis, the liver appears to be amongst the first organs affected as the liver macrophages (Kupffer cells) have been shown to play a key role in the removal of xenobiotics from the blood [5]. It is well documented that LPS stimulation of the Kupffer cells results in the release various cytokines/chemokines including TNF-α, IL-6, HMGB1, and nitric oxide (NO) [6], which have been shown to induce SIRS development [7,8].

The factors regulating the release of cytokines from macrophages are not fully understood although it has been hypothesized that this process is regulated, at least in part, by increases in cellular ROS which has led some to hypothesize that the use of antioxidants may be valuable for the treatment of sepsis [9–11]. Although promising in animals, the vast majority of interventional studies examining the effects of antioxidant therapies have been largely ineffective in clinical trials [12]. The reasons for these failures are currently unknown and likely complex in nature but may be related to the fact that the treatment of sepsis is oftentimes hindered by the sepsis-associated circulatory abnormalities, poor bio-distribution, and individual differences in the septic presentation. In addition, the use of traditional pharmacological approaches can be limited by the need for multiple daily dosing since each anti oxidant molecule is typically capable of scavenging only one free radical [13]. In an effort to overcome these limitations, we sought to develop a treatment that would not only target the liver Kupffer cells which are responsible for initiating SIRS development, but one that was also capable of exhibiting continued activity over time.

Ceria is a rare earth element of the lanthanide series that is used in automobile catalytic converters to convert carbon monoxide to carbon dioxide [14]. In its oxide form, ceria can transition between Ce^{3+} and Ce^{4+} oxidative states which can allow for auto regenerative redox cycling and free radical scavenging [13]. Although the use of CeO_2 in nanoparticle form for biomedical applications awaits further development, previous reports have indicated that these particles possess antioxidative activity [14] and that they tend to accumulate in the Kuppfer cells when injected into the systemic circulation of the laboratory rat [15]. On the basis of these data, we hypothesized that the systemic administration of CeO_2 nanoparticles would be associated with diminished Kupffer cell cytokine/chemokine release and decreased SIRS development which would result in improved animal survival following sepsis insult.

2. Material and methods

2.1. Cerium oxide nanoparticle preparation and characterization

The CeO_2 nanoparticles were purchased from Sigma–Aldrich (USA) and characterized as outlined. Stock suspensions (3.5 mg/ml) were prepared in ddH2o by sonication (600 W for 2 min) using a Vibra Cell Sonicator (Sonics & Materials, Inc.) at room temperature and characterized. Dynamic light scattering (DLS) was performed to estimate the mean size of CeO_2 NPs in suspension using LB-550 DLS particle size analyzer (Horiba Scientific, Edison, NJ). Naked particle size of the CeO_2 NPs was characterized by transmission electron microscopy (TEM) using JEOL JEM 1200Ex. X-ray diffraction (XRD) was performed using a Scintag XDS 2000 powder diffractometer. Scanning transmission electron microscopy (STEM) images were acquired using a JEM-ARM200CF (JEOL, Japan) operated at 200 keV. The oxidative state of cerium was analyzed by X-ray photoelectron spectroscopy (XPS) using a PHI ESCA 5400 spectrophotometer.

2.2. Animal preparation and experimental design

Animals were prepared for experiments as detailed in the Selvaraj et al. [16] and were randomly assigned to one of four groups. The control group (n = 6) received 1.5 ml of endotoxin free water by i.p. while the CeO_2 nanoparticle treated group (n = 6) received 1.5 ml of endotoxin free water by i.p. and CeO_2 nanoparticles (0.5 mg/kg) in 200 μl of sterile distilled water via the tail vein. The LPS treated group (n = 12) received LPS (055-B5; 40 mg/kg, Sigma, St. Louis, MO) in 1.5 ml of sterile water by i.p. and 200 μl of sterile distilled water via the tail vein while the LPS + CeO_2 NPs treatment group received LPS (40 mg/kg) in 1.5 ml of sterile water by i.p. and CeO_2 nanoparticles (0.5 mg/kg) in 200 μl of sterile distilled water via the tail vein. The animal survival rate was assessed for a period of 7 days. LPS-induced sepsis symptoms were quantitated by monitoring animal behavior, body temperature and respiratory rate using a Mouse Ox Plus from Star Scientific Corp (Massachusetts, USA), while heart rate and blood pressure were evaluated using a CODA blood pressure system from Kent Scientific (Connecticut, USA).

2.3. Sample collection, estimation of blood cell number and quantification of serum cytokines

In an additional set of experiments, blood and livers were collected at 6 or 24 h after study initiation. Differential blood cells were estimated in whole blood using an Abaxis VetScan HM2 hematology analyzer (Abaxis, Union city, CA). Serum TNF-α levels were analyzed by enzyme-linked immunosorbent assay (ELISA) (BD Bioscience, Franklin Lakes, NJ). Serum samples from each of the different groups (n = 6/group) were pooled and sent to Myriad RBM (Austin, TX) for the analysis of cytokines, chemokines and markers of inflammation using rodent MAP® V. 3.0 as detailed elsewhere [17,18]. Nitrite in the serum was assayed using the Griess reaction using a kit from Cayman Chemical Company (Ann Arbor, Michigan, USA).

2.4. Estimation of CeO_2 nanoparticle content in the liver and analysis of liver damage

Liver ceria content was estimated by induction coupled plasma-mass spectrometry (ICP-MS) as described elsewhere [18]. In other experiments, portions of each liver were formalin fixed, sectioned, and stained with hematoxylin and eosin (H&E) for histopathological examination. Microscopic images were captured using an EVOS XL Core microscope (Fisher Scientific, Pittsburgh, PA, USA). Liver damage markers in the serum were estimated using an Abaxis VetScan analyzer (Abaxis, UnionCity, CA) and Myriad RBM (Austin, TX).

2.5. Immunoblotting and TUNEL staining

Proteins samples were prepared from the liver for immunoblotting as detailed in Selvaraj et al. [16]. Liver cell apoptosis was assessed using a transferase-mediated dUTP nick-end labeling (TUNEL) kit (Roche Applied Science, Indianapolis, IN) as described in Selvaraj et al. [16].

2.6. Kupffer cell isolation and assays

Kupffer cells were isolated from rat liver and purified by differential centrifugation using a Percoll gradient as described previously [19]. The purity of the KCs was determined by ED1 and ED2 staining (immunofluorescence) as described [7]. KCs were cultured and treated with LPS in the presence and absence of CeO_2 nanoparticles for 24 h and TNF-α release was measured by ELISA. Reactive oxygen species (ROS) levels were determined using the OxiSelect™ kit from Cell Bio Labs (San Diego, CA), as outlined by the manufacturer.

2.7. Macrophage uptake of CeO_2 nanoparticles and effect against LPS challenge

The cytotoxic and protective effect of CeO_2 nanoparticles against LPS challenge was determined by the MTT assay as described in Selvaraj et al. [16]. CeO_2 nanoparticle uptake by the macrophage cells was estimated by inductively coupled plasma-mass spectrometry (ICP-MS) at Elementary Analysis Inc (Lexington, Kentucky, USA) as described previously [20].

ROS levels were determined using the OxiSelect™ kit from Cell Bio Labs (San Diego, CA) while mitochondrial membrane damage was estimated by $\Delta\psi m$ using the JC 1 dye (Cell Technology, Mountain View, CA) as described elsewhere [21]. Nitrite production was assayed using the Griess reaction kit from Cayman Chemical Company (Ann Arbor, Michigan, USA) as described by the manufacturer. The concentration of TNF-α, IL-6, IL-1β and HMGB1 in the media was measured by ELISA reagent kits as described in Selvaraj et al. [16].

2.8. Electromobility shift and luciferase reporter assays

The electromobility shift (EMSA) assay was performed using a commercially available kit (Pierce, Rockford, IL, USA) as described in Selvaraj et al. [16]. Luciferase reporter assays were performed using a NF-kB reporter construct from Promega (Madison, WI, USA) as detailed in Selvaraj et al. [16].

2.9. Statistical analysis

Data are presented as mean ± standard error of the mean (SEM). Dependent variables were analyzed by one way ANOVA by Holm-Sidak test using SigmaStat (Aspire Software International, Auburn VA) and *post-hoc* testing where appropriate. A $P < 0.05$ was considered as significant.

3. Results

3.1. Characterization of CeO_2 nanoparticle

SEM and TEM analysis determined the size of individual nano-particles to be between 200 and 400 nm (Fig. 1A(i, ii)). The mean hydrodynamic diameter of CeO_2 nanoparticles as estimated by dynamic light scattering was 53.36 ± 7.04 nm (Fig. 1B(i)). XRD spectral analysis confirmed the purity of CeO_2 nanoparticles preparation and demonstrated well defined peaks 2Θ = 28.5, 33.1, 47.5, 56.2, 59.0 and 69.2. No other peaks related to impurities were detected (Fig. 1B(ii)). XSP spectral analysis indicated a higher concentration of Ce^{4+} than Ce^{3+} in the CeO_2 nanoparticles (Fig. 1C(i)).

3.2. Effect of CeO_2 nanoparticle treatment on animal mortality and physiological function

Nanoparticle treatment decreased LPS-induced mortality from 70 % to 10 % (Fig. 1C(ii), $P < 0.05$). Increases in animal survivability were associated with improvements in animal behavior (Selvaraj et al. Table 1 [16]), core body temperature (Fig. 1D(i), $P < 0.05$), decreased respiratory rate (Fig. 1D(ii)), and increases in blood pressure (Fig. 1E). Sepsis decreased the percentage of lymphocytes and increased the percentage of granulocytes at 6 and 24 h. Nanoparticle treatment reversed these changes at the 6 h time point (Selvaraj et al. Table 2 $P < 0.05$ [16]).

3.3. Nanoparticle treatment decrease sepsis related systemic inflammation

Compared to controls, LPS-induced sepsis was associated with increased serum cytokines, chemokines and acute phase proteins including tumor necrosis factor alpha (TNF-α), interleukin-1 beta (IL-1β), interleukin-1 alpha (IL-1α) at 6 h ($P < 0.05$). Nanoparticle treatment decreased serum TNF-α, IL-1β levels at 6 h and IL-1α at both 6 and 24 h (Fig. 2A(i,ii) and B(i), $P < 0.05$). Compared to controls, LPS-induced sepsis appeared to increase the amount of macrophage derived chemokine (MDC), macrophage inflammatory protein-1 beta (MIP-1 β), macrophage inflammatory protein-2 (MIP-2), macrophage inflammatory protein-3 beta (MIP-3 β), macrophage inflammatory protein-1 alpha (MIP-1 α), monocyte chemotactic protein-1 (MCP-1), monocyte chemotactic protein-3 (MCP-3), granulocyte chemotactic protein 2 (GCP-2), and growth regulated alpha protein (KC/GROα)at 6 and 24 h (Fig. 2B(ii) to F(ii)). Nanoparticle administration decreased the levels of MIP-2, MIP-3β, MCP-1, MCP-3, GCP-2 and KC/GROα at both 6 and 24 h ($P < 0.05$) (Fig. 2C(ii) to F(ii)). The expression of several other acute phase and inflammatory proteins including stem cell factor, myoglobin, CD-40 ligand, fibrinogen, growth hormone, heptaglobin, leptin, and interferon gamma induced protein 10 (IF-10) were also altered with sepsis and with treatment (Selvaraj et al. Table 3 [16]).

3.4. Nanoparticle treatment increase liver ceria content and protects the liver against sepsis induced damage

Compared to untreated animals, liver ceria content was increased in the nanoparticle injected animals (Fig. 3A(ii)). Sepsis associated decreases in liver weight were attenuated with nanoparticle treatment (Fig. 3A(iii), $P < 0.05$). Histological analyses of the livers obtained from control animals were unremarkable. Sepsis was associated with changes in cell swelling, inflammation, necrosis, sinusoidal dilatation and the infiltration of cells in the portal area (Fig. 3B) which appeared to be diminished with nanoparticle treatment. Consistent with these changes in liver histology, sepsis was found to increase serum bilirubin (TBIL) at 24 h while serum alanine aminotransferase (ALT), glutathione S-transferase Mu (GST-Mu), and glutathione S-transferase alpha (GST-α) levels were elevated at 6 and 24 h. Nanoparticle treatment decreased serum bilirubin, ALT, GST-Mu, and GST-α (Fig. 3C (i to iii) and D(i), $P < 0.05$).

3.5. Nanoparticle treatment decrease sepsis related increase in MyD88, MAPK activation, iNOS and HMGB1

Compared to that seen in the control animals, sepsis increased the expression of MyD 88, and the phosphorylation of p38-MAPK and p44/42-MAPK which were decreased with nanoparticle treatment (Fig. 3D(ii) and E(i, ii), $P < 0.05$). Sepsis increased serum nitrite levels at 6 and 24 h. Nanoparticle treatment decreased LPS-induced nitrite production (Fig. 3A (i)) along with LPS associated increases in liver iNOS and HMBG-1 content (Fig. 4A(i, ii), $P < 0.05$).

3.6. Nanoparticle treatment decrease hepatic apoptosis during sepsis

To investigate the possibility that changes in liver structure were associated with cellular apoptosis we determined the number of nuclei staining positively for DNA fragmentation by TUNEL staining. As expected, we found that sepsis increased and that nanoparticle treatment decreased the number of TUNEL positive nuclei (Fig. 4A (iii), Fig. 4B, $P < 0.05$). These decreases in cellular apoptosis with treatment were associated with decreased caspase-3 cleavage (19 and 17-kDa fragments) (Fig. 4C (i), $P < 0.05$) and a decrease in the Bax/Bcl-2 ratio (Fig. 4C (ii), $P < 0.05$).

3.7. Nanoparticle treatment decrease LPS-induced increase in macrophage ROS level and cytokine release

Based on the fact that many of the cytokines/chemokines and other inflammatory regulators observed during SIRS are likely derived from the liver Kupffer cells [22] and from our serum profiling data (Fig. 2 and Selvaraj et al. Table 3 [16]) we next examined the effect of LPS challenge on Kupffer cell function in the absence and presence of CeO_2 nanoparticles. Compared to control cells, LPS challenge was associated with alterations in cellular morphology, increased TNF-α production, and elevations in cellular ROS levels which appeared to be diminished with nanoparticle treatment (Fig. 4D, C(iii) and E).

Because of the difficulties associated with the continued propagation of Kuppfer cells in culture we next examined the effects of nanoparticle treatment in depth using cultured

RAW264.7 macrophages. Dose response toxicity experiments using the MTT assay suggested that nanoparticle dosages greater than 1 μg/ml appeared to be cytotoxic (Selvaraj et al. [16] Fig. 1, $P < 0.05$). Consistent with our *in vivo* data, LPS-induced increases in cell death were diminished with nanoparticle treatment (25, 50,100 or 1000 ng/ml) (Fig. 5A (i), $P < 0.05$). To test if the improvements in cell survival were associated with the ability of the nanoparticles to bind to/sequester LPS or if exposure to the nanoparticles was able to neutralize LPS functionality, varying doses of CeO_2 nanoparticles (0,1, 5,10, 25, 50,100, or 1000 ng/ml) were added to growth media containing LPS (2 μg/ml) and allowed to interact. After centrifugation to remove any suspended nanoparticles, the MTT assay was performed using the clarified media. Consistent with the possibility that the nanoparticles do not act to impair LPS functionality, we did not observe any differences in the amount of cell death caused between incubation of the cells with “native” and nanoparticle “exposed” LPS (Fig. 5 A (ii)). The uptake of CeO_2 nanoparticles by the RAW264.7 cells in the presence or absence of LPS was confirmed using ICP-MS (Fig. 5)B(i).

To investigate whether changes in cell survival were associated with alterations in cellular ROS, RAW264.7 cells were stained with DCFH-DA and JC-1 dyes to determine the effects of nanoparticle treatment on cellular superoxide levels and mitochondrial membrane potential ($\Delta\psi m$) levels, respectively [23,24]. As might be expected given the potential ROS scavenging ability of CeO_2 nanoparticles [13,14], nanoparticle treatment was found to decrease LPS-induced increases in cellular ROS and mitochondrial membrane potential (Fig. 6A (i,ii), $P < 0.05$).

In addition to changes in cellular ROS, nanoparticle treatment also decreased the production of TNF-α, IL-6, IL-1β, and HMGB1 following LPS challenge (Fig. 5B (ii) to D(i), $P<0.05$). Similarly, nanoparticle treatment also decreased nitrite production, along with the upregulation of iNOS and COX-2 protein following LPS challenge (Fig. 5D(ii) to E(i,ii), ($P < 0.05$)).

3.8. Nanoparticle treatment decrease NF-kB/p65 transcriptional activity

LPS-induced decreases in I_kB-α protein were abrogated following nanoparticle treatment (Fig. 6B (i), $P < 0.05$). Consistent with these data, nanoparticle treatment also decreased LPS-induced translocation of NF-kB/p65 to the nucleus (Fig. 6B (ii), C(i)), NF-kB/p65 binding to DNA (Figure C(ii), D(i)), and LPS-associated increases in NF-kB transcriptional activity (Fig. 6D (ii), $P < 0.05$).

4. Discussion

Despite decades of intensive investigation and significant advances in medical technology, the overall mortality rate in severe sepsis patients remains unacceptably high. The aim of this study was to evaluate whether CeO_2 nanoparticles are protective against LPS-induced sepsis in the Sprague Dawley rat. The primary finding of this study was that a single injection of CeO_2 nanoparticles, in the absence of antibiotic treatment, fluid resuscitation, or other pharmacological intervention, was able to increase animal survivability 200% following a severe septic insult (Fig. 1C (ii)).

Consistent with previous studies we found that severe sepsis was associated with changes in body temperature, respiratory rate, and blood pressure and blood cell counts [2,25,26]. Nanoparticle treatment attenuated sepsis-induced changes in these variables (Fig. 1D (i,ii), and E)). Given that serum cytokine/chemokine levels are highly correlated with patient survival [27] we next sought to determine if the nanoparticle treatment functioned to diminish SIRS development. As expected, we found that sepsis was associated with the significant upregulation of a number of different cytokines, chemokine, acute phase proteins, and other inflammatory mediators and importantly, that the nanoparticle treatment appeared to significantly blunt many of these sepsis-induced changes (Fig. 2 and Selvaraj et al. Table 3 [16]). These latter data are in agreement with the previous work of Kyosseva and colleagues who demonstrated that a single injection of nanoceria in the neurodegeneration prone Vldlr–/– mouse was able to attenuate the expression of several proinflammatory cytokines and proangiogenic growth factors [28].

To explore the mechanistic basis of this finding, we next determined where the injected CeO2 nanoparticles may accumulate. Similar to previous work [29], ICP-MS analysis demonstrated significantly higher amounts of ceria in the livers of the treated animals compared to that observed in the untreated animals (Fig. 3A (ii)). To examine if the CeO2 nanoparticles were able to protect the liver injury against a septic insult we next examined if treatment was associated with improvement in liver structure and function. We observed that sepsis was associated with alterations in liver morphology (Fig. 3B) and evidence of diminished function as suggested by increased serum bilirubin levels (Fig. 3C (i)). In addition, we found that the LPS treated animals exhibited increased serum levels of the liver damage molecules alanine aminotransferase (ALT), glutathione S-transferase Mu (GST Mu), glutathione S-transferase alpha (GST-α), (Fig. 3C (ii, iii) and D(i)). Importantly, each of these measures were decreased significantly with nanoparticle treatment (Fig. 3C (i-iii) and D(i)). Supporting these data, we also found that the nanoparticle treatment was associated with diminished hepatic MyD88 levels, p-p38 MAPK phosphorylation, p-ERK1/2, iNOS, and HMGB-1 suggesting that nanoparticle treatment was also associated with decreased liver inflammation (Fig. 3D (ii), E(i,ii) and Fig. 4 A(i,ii)). These data are consistent with the previous work of Cai et al. [30], and Kyosseva and co-workers [28] who also demonstrated that the administration of nanoceria was associated with decreased evidence of cellular inflammation and the attenuation of MAPK phosphorylation. To extend these findings we next examined if the nanoparticle treatment was also able to protect the liver from sepsis-induced apoptosis. As expected, we found that the nanoparticle treatment was associated with a diminished number of TUNEL positive hepatic nuclei, decreased caspase-3 cleavage, and a reduction in the Bax/Bcl-2 ratio (Fig. 4A (iii) 4B, and C (i-ii)).

Given that many of cytokines and chemokines (e.g. TNF-α, IL-6, MDC, MIP-1β, MIP-2, MIP-3β, MCP-3, KC/GROα) that we found to be elevated with sepsis and decreased with treatment are thought to be derived from the liver Kuppfer cells (macrophages) [5,31], we next examined the function of these particles in isolated Kupffer cells. We found that nanoparticle treatment was associated with decreased TNF-α release and cellular ROS levels after LPS challenge (Fig. 4C (iii) and E). Using cultured RAW264.7 macrophages which we could easily propagate, we repeated this experimental approach and found that the nanoparticle treatment decreased LPS-induced increases in the secretion of TNF-α, IL-6,

IL-1β and HMGB1 (Fig. 5B (ii) to D (i)). In addition to elevations in cytokine concentration, it has also been suggested that the large amount of nitric oxide (NO) produced during sepsis may play an important role in sepsis-induced mortality which has led some to postulate that decreasing NO levels may be beneficial [32,33]. Our *in vivo* and *in vitro* data show a significant decrease in the NO production in serum as well as cultured macrophages following nanoparticle treatment (Fig. 3A (i) and Fig. 5D (ii)). To confirm this finding, we next examined how CeO_2 nanoparticle affected the expression of inducible nitric oxide synthase (iNOS) which is the enzyme thought to be responsible for much of the NO produced during the septic insult. Paralleling our findings of decreased serum nitrite (Fig. 3A (i)) and diminished iNOS levels (Fig. 4A (i)) in the livers of the nanoparticle treated animals, we found that the nanoparticles also diminished LPS-induced expression of iNOS in cultured macro-phages (Fig. 5E (i)).

The mechanism(s) regulating cytokine and NO production in macrophages following LPS stimulation are not yet fully understood, however recent data has suggested that elevations in intracellular ROS levels may play an important role [34]. To examine this possibility, we next determined how nanoparticle treatment might affect cellular ROS and mitochondrial membrane potential levels by DCFH-DA and JC-1 staining. Consistent with previous reports using macrophages [35–37], we found that CeO_2 nanoparticle treatment tended to decrease the induction of cellular ROS in RAW macro-phage cells and mitochondrial membrane potential damage following LPS challenge (Fig. 6A (i, ii)).

It is thought that NF-kB and mitogen activated protein kinases (MAPK) are key regulators of inflammatory gene expression [38]. Although the factors regulating NF-kB transcriptional activity are not fully understood, it is well known that nuclear localization of the redox sensitive NF-kB transcription factor is controlled by the phosphorylation and subsequent degradation of I_kB-α [35]. It has been reported that LPS challenge (2 μg/ml) can be used to induce the degradation of I_kB-α and nuclear localization of NF-kB/p65 in cultured RAW264.7 macrophages [39,40]. Consistent with our previous data, we found that nanoparticle treatment functioned to attenuate LPS-induced I_kB-α degradation and NF-kB/p65 trans-location from the cytoplasm to the nucleus (Fig. 6B (i,ii) and C(i)). Importantly, we also noted that these decreases in NF-kB trans-location were also associated with diminished NF-kB binding to DNA (Fig. 6C (ii) and D (i)) and reduced NF-kB transcriptional activation (Fig. 6D(ii) $P < 0.05$).

5. Conclusion

In summary, our data suggest that a single dose of CeO_2 nanoparticles is associated with improvements in animal survival, decreased hepatic damage, increased ceria deposition in the liver, and diminished evidence of systemic inflammation after a severe septic insult. *In vitro* experimentation using isolated Kupffer cells and cultured RAW264.7 macrophages demonstrated that CeO_2 nanoparticle treatment decreased cytokine release (TNF-α, IL-1 β, IL-6, HMGB1), the induction of iNOS, NF-kB transcriptional activity following LPS challenge (Selvaraj et al. [16] Fig. 1), and MAPK (Selvaraj et al. [41] Fig. 1). Given that the large scale manufacture of these particles is possible using existing technology and their likely stability under a wide range of environmental conditions it is possible that these

particles may have application for the treatment of sepsis in austere environments. Additional studies examining the potential efficacy of CeO_2 nanoparticles for the treatment of sepsis may be warranted.

Acknowledgments

This work was supported in part from DOE grant (DE-PS02-09ER-01 to E.R.B).

References

1. Angus DC, Linde-Zwirble WT, Lidicker J, Clermont G, Carcillo J, Pinsky MR. Epidemiology of severe sepsis in the United States: analysis of incidence, outcome, and associated costs of care. Crit care Med. 2001; 29:1303–1310. [PubMed: 11445675]
2. Annane D, Bellissant E, Cavaillon JM. Septic shock. Lancet. 2005; 365:63–78. [PubMed: 15639681]
3. Larrosa M, Azorin-Ortuno M, Yanez-Gascon MJ, Garcia-Conesa MT, Tomas-Barberan F, Espin JC. Lack of effect of oral administration of resveratrol in LPS-induced systemic inflammation. Eur J Nutr. 2011; 50:673–680. [PubMed: 21373948]
4. Wang D, Yin Y, Yao Y. Advances in sepsis-associated liver dysfunction. Burns Trauma. 2:97–105.
5. Granado M, Martin AI, Priego T, Villanua MA, Lopez-Calderon A. Inactivation of Kupffer cells by gadolinium administration prevents lipopolysaccharide-induced decrease in liver insulin-like growth factor-I and IGF-binding protein-3 gene expression. J Endocrinol. 2006; 188:503–511. [PubMed: 16522730]
6. Kolios G, Valatas V, Kouroumalis E. Role of Kupffer cells in the pathogenesisof liver disease. World J Gastroenterol WJG. 2006; 12:7413–7420. [PubMed: 17167827]
7. Zeng WQ, Zhang JQ, Li Y, Yang K, Chen YP, Liu ZJ. A new method to isolateand culture rat Kupffer cells. PLoS One. 2013; 8:e70832. [PubMed: 23967115]
8. Paterson RL, Webster NR. Sepsis and the systemic inflammatory responsesyndrome. J R Coll Surg Edinb. 2000; 45:178–182. [PubMed: 10881485]
9. Kim TH, Yoon SJ, Lee SM. Genipin attenuates sepsis by inhibiting toll-like receptor signaling. Mol Med. 2012; 18:455–465. [PubMed: 22252713]
10. Villa P, Ghezzi P. Effect of N-acetyl-L-cysteine on sepsis in mice. Eur J Pharmacol. 1995; 292:341–344. [PubMed: 7796876]
11. Zapelini PH, Rezin GT, Cardoso MR, Ritter C, Klamt F, Moreira JC, et al. Antioxidant treatment reverses mitochondrial dysfunction in a sepsis animal model. Mitochondrion. 2008; 8:211–218. [PubMed: 18417427]
12. Rahman I. Pharmacological antioxidant strategies as therapeutic interventions for COPD. Biochim Biophys Acta. 2012; 1822:714–728. [PubMed: 22101076]
13. Niu J, Wang K, Kolattukudy PE. Cerium oxide nanoparticles inhibit oxidative stress and nuclear factor-kappaB activation in H9c2 cardiomyocytes exposed to cigarette smoke extract. J Pharmacol Exp Ther. 2011; 338:53–61. [PubMed: 21464334]
14. Celardo I, Pedersen JZ, Traversa E, Ghibelli L. Pharmacological potential of cerium oxide nanoparticles. Nanoscale. 2011; 3:1411–1420. [PubMed: 21369578]
15. Tseng MT, Fu Q, Lor K, Fernandez-Botran GR, Deng ZB, Graham U, et al. Persistent hepatic structural alterations following nanoceria vascular infusion in the rat. Toxicol Pathol. 2014; 42:984–996. [PubMed: 24178579]
16. Selvaraj V, Nepal N, Rogers S, Manne N, Arvapalli R, Rice K, et al. Cerium oxide nanoparticles inhibit lipopolysaccharide induced MAP kinase/NF-kB mediated severe sepsis. Data in Brief. 2015 In press.
17. Casrouge A, Decalf J, Ahloulay M, Lababidi C, Mansour H, Vallet-Pichard A, et al. Evidence for an antagonist form of the chemokine CXCL10 in patients chronically infected with HCV. J Clin Invest. 2011; 121:308–317. [PubMed: 21183794]

18. Nalabotu SK, Kolli MB, Triest WE, Ma JY, Manne ND, Katta A, et al. Intratracheal instillation of cerium oxide nanoparticles induces hepatic toxicity in male Sprague-Dawley rats. Int J Nanomedicine. 2011; 6:2327–2335. [PubMed: 22072870]
19. Selvaraj V, Sampath K, Sekar V. Administration of yeast glucan enhances survival and some non-specific and specific immune parameters in carp (Cyprinus carpio) infected with *Aeromonas hydrophila*. Fish Shellfish Immunol. 2005; 19:293–306. [PubMed: 15863011]
20. Patil S, Sandberg A, Heckert E, Self W, Seal S. Protein adsorption and cellular uptake of cerium oxide nanoparticles as a function of zeta potential. Bio-materials. 2007; 28:4600–4607.
21. Selvaraj V, Armistead MY, Cohenford M, Murray E. Arsenic trioxide (As(2) O(3)) induces apoptosis and necrosis mediated cell death through mitochondrial membrane potential damage and elevated production of reactive oxygen species in PLHC-1 fish cell line. Chemosphere. 2013; 90:1201–1209. [PubMed: 23121984]
22. Jaeschke H, Williams CD, Ramachandran A, Bajt ML. Acetaminophen hepatotoxicity and repair: the role of sterile inflammation and innate immunity. Liver Int. 2012; 32:8–20. [PubMed: 21745276]
23. Woo CH, Lim JH, Kim JH. Lipopolysaccharide induces matrix metalloproteinase-9 expression via a mitochondrial reactive oxygen species-p38 kinase-activator protein-1 pathway in RAW 264.7 cells. J Immunol. 2004; 173:6973–6980. [PubMed: 15557194]
24. Yu LC, Flynn AN, Turner JR, Buret AG. SGLT-1-mediated glucose uptake protects intestinal epithelial cells against LPS-induced apoptosis and barrier defects: a novel cellular rescue mechanism? FASEB J. 2005; 19:1822–1835. [PubMed: 16260652]
25. Bone RC, Balk RA, Cerra FB, Dellinger RP, Fein AM, Knaus WA, et al. Definitions for sepsis and organ failure and guidelines for the use of innovative therapies in sepsis. The ACCP/SCCM Consensus Conference Committee. American College of Chest Physicians/Society of Critical Care Medicine. Chest. 1992; 101:1644–1655. [PubMed: 1303622]
26. Merx MW, Weber C. Sepsis and the heart. Circulation. 2007; 116:793–802. [PubMed: 17698745]
27. Oda S, Hirasawa H, Shiga H, Nakanishi K, Matsuda K, Nakamua M. Sequential measurement of IL-6 blood levels in patients with systemic inflammatory response syndrome (SIRS)/sepsis. Cytokine. 2005; 29:169–175. [PubMed: 15652449]
28. Kyosseva SV, Chen L, Seal S, McGinnis JF. Nanoceria inhibit expression of genes associated with inflammation and angiogenesis in the retina of vldlr null mice. Exp Eye Res 116. 2013:63–74.
29. Hirst SM, Karakoti A, Singh S, Self W, Tyler R, Seal S, et al. Bio-distribution and in vivo antioxidant effects of cerium oxide nanoparticles in mice. Environ Toxicol. 2013; 28:107–118. [PubMed: 21618676]
30. Cai X, Seal S, McGinnis JF. Sustained inhibition of neovascularization in vldlr-/- mice following intravitreal injection of cerium oxide nanoparticles and the role of the ASK1-P38/JNK-NF-kappaB pathway. Biomaterials. 2014; 35:249–258. [PubMed: 24140045]
31. Sun D, Chen D, Du B, Pan J. Heat shock response inhibits NF-kappaB activation and cytokine production in murine Kupffer cells. J Surg Res. 2005; 129:114–121. [PubMed: 16243048]
32. Stoclet JC, Muller B, Andriantsitohaina R, Kleschyov A. Overproduction of nitric oxide in pathophysiology of blood vessels. Biochem (Mosc). 1998; 63:826–832.
33. Suh N, Honda T, Finlay HJ, Barchowsky A, Williams C, Benoit NE, et al. Novel triterpenoids suppress inducible nitric oxide synthase (iNOS) and inducible cyclooxygenase (COX-2) in mouse macrophages. Cancer Res. 1998; 58:717–723. [PubMed: 9485026]
34. Lee SY, Kim HJ, Han JS. Anti-inflammatory effect of oyster shell extract in LPS-stimulated Raw 264.7 cells. Prev Nutr food Sci. 2013; 18:23–29. [PubMed: 24471106]
35. Tsai YY, Oca-Cossio J, Agering K, Simpson NE, Atkinson MA, Wasserfall CH, et al. Novel synthesis of cerium oxide nanoparticles for free radical scavenging. Nanomedicine (Lond). 2007; 2:325–332. [PubMed: 17716177]
36. Niu J, Azfer A, Rogers LM, Wang X, Kolattukudy PE. Cardioprotective effects of cerium oxide nanoparticles in a transgenic murine model ofcardiomyopathy. Cardiovasc Res. 2007; 73:549–559. [PubMed: 17207782]
37. Hirst SM, Karakoti AS, Tyler RD, Sriranganathan N, Seal S, Reilly CM. Anti-inflammatory properties of cerium oxide nanoparticles. Small. 2009; 5:2848–2856. [PubMed: 19802857]

38. Powers SK, Talbert EE, Adhihetty PJ. Reactive oxygen and nitrogen species as intracellular signals in skeletal muscle. J Physiol. 2011; 589:2129–2138. [PubMed: 21224240]

39. Grossman BJ, Shanley TP, Odoms K, Dunsmore KE, Denenberg AG, Wong HR. Temporal and mechanistic effects of heat shock on LPS-mediated degradation of IkappaBalpha in macrophages. Inflammation. 2002; 26:129–137. [PubMed: 12083419]

40. Cheng PY, Lee YM, Wu YS, Chang TW, Jin JS, Yen MH. Protective effect of baicalein against endotoxic shock in rats in vivo and in vitro. Biochem Pharmacol. 2007; 73:793–804. [PubMed: 17182007]

41. Selvaraj V, Nepal N, Rogers S, Manne N, Arvapalli R, RIce K, et al. Lip-oplysaccharide induced MAP kinase activation in RAW 264.7 cells attenuated by cerium oxide nanoparticles. Data in Brief. 2015 In press.

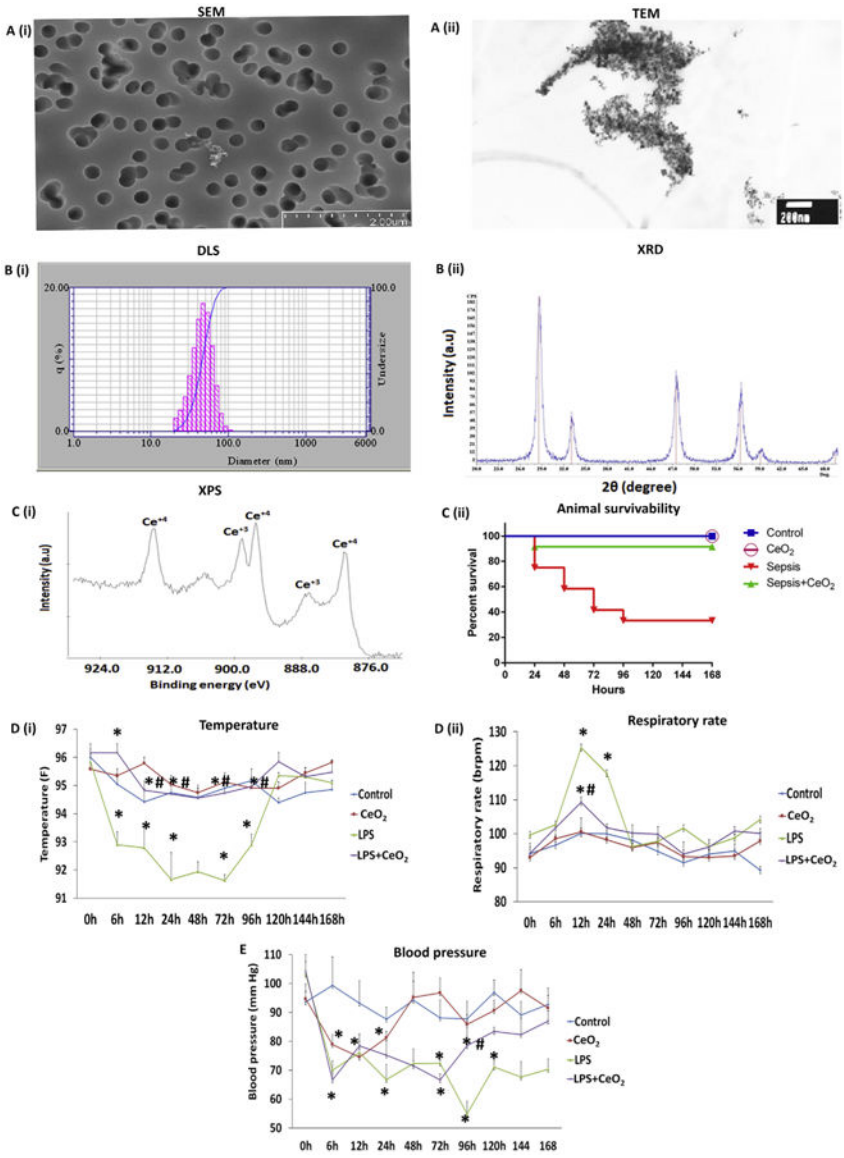

Fig. 1. Characterization of CeO_2 nanoparticles, animal survivability and physiological changes

A (i) Scanning electron microscopy (SEM) image of CeO_2 nanoparticles, A (ii) Transmission electron microscopy (TEM) image of CeO_2 nanoparticles, B (i) Dynamic light scattering (DLS) image of CeO_2 nanoparticles, B (ii) X-ray diffraction image of CeO_2 nanoparticles, and C (i) X-ray photoelectron spectroscopy image of CeO_2 nanoparticles. C (ii) Animal survivability of control (vehicle only, n = 6), CeO_2 nanoparticle treated (0.5 mg/kg, n = 6), sepsis (40 mg/kg of LPS, n = 16), and sepsis + CeO_2 nanoparticle treatment (40 mg/kg of LPS + 0.5 mg/kg of CeO_2 nanoparticles (n = 16)), D (i) Temperature, D (ii) Respiratory rate, and (E) Blood pressure. $*P < 0.05$ compared to control group, $*^{\#}P < 0.05$ compared to LPS group.

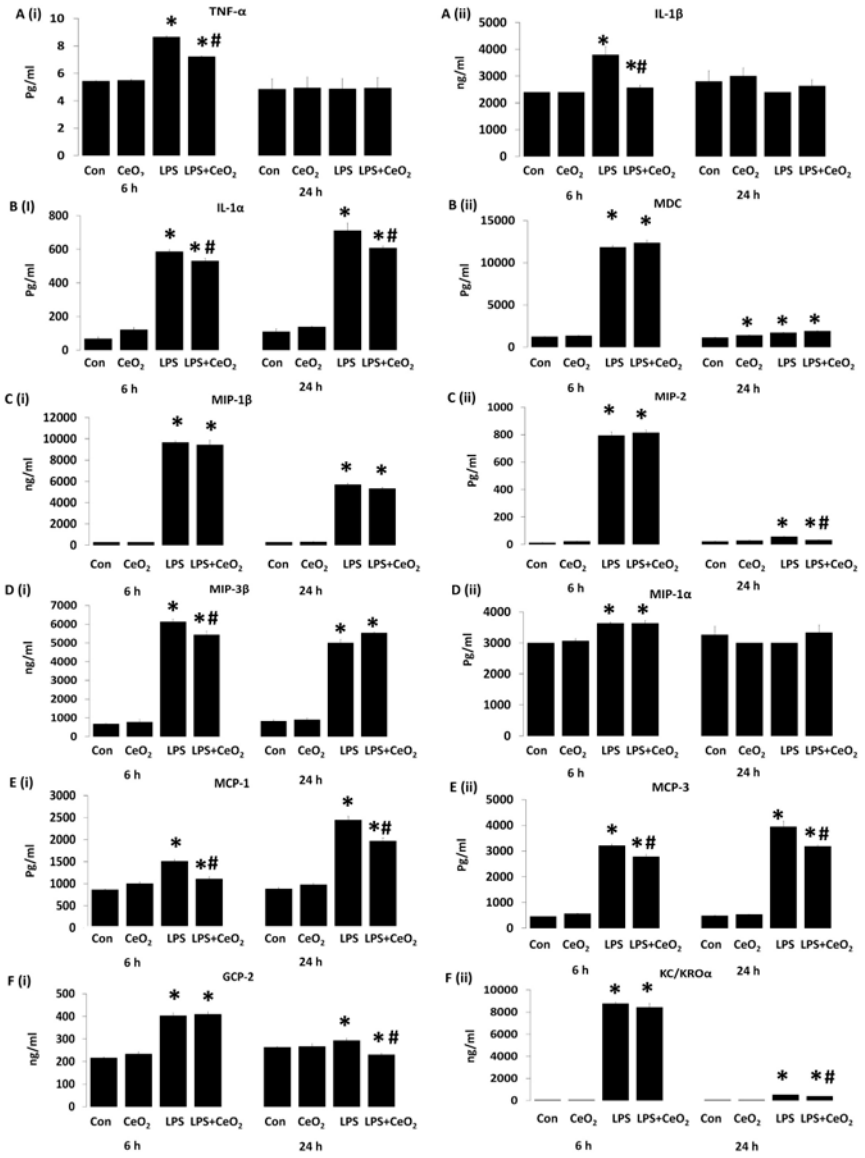

Fig. 2. Effect of CeO_2 nanoparticles on LPS induced alteration of serum cytokines and chemokines

Cytokines changes: A (i) Tumor necrosis factor alpha (TNF-α), A (ii) interleukin 1 beta (IL-1β), B (i) Interleukin 1 alpha (IL-1α). Chemokines changes: B (ii) macrophage derived chemokines (MDC), C (i) macrophage inflammatory protein 1 beta (MIP-1β), C (ii) macrophage inflammatory protein-2 (MIP-2), D (i) macrophage inflammatory protein-3 beta (MIP-3β), D (ii) macrophage inflammatory protein-1 alpha (MIP-1α), E (i) monocyte chemotactic protein-1 (MCP-1), E (ii) monocyte chemotactic protein-3 (MCP-3), F (i) granulocytes chemotactic protein (GCP-2), and F (ii) growth regulated alpha protein (KC/GROα). Serum samples were pooled from control (n = 6), CeO_2 (n = 6), Sepsis (n = 6), Sepsis + CeO_2 (n = 6) and analyzed in triplicate. Values are mean ± SEM of 3 independent experiments performed in triplicate. Statistical significance was determined by a one way ANOVA using Holm–Sidak test. $^{*}P < 0.05$ compared to control group, $^{*\#}P < 0.05$ compared to LPS group.

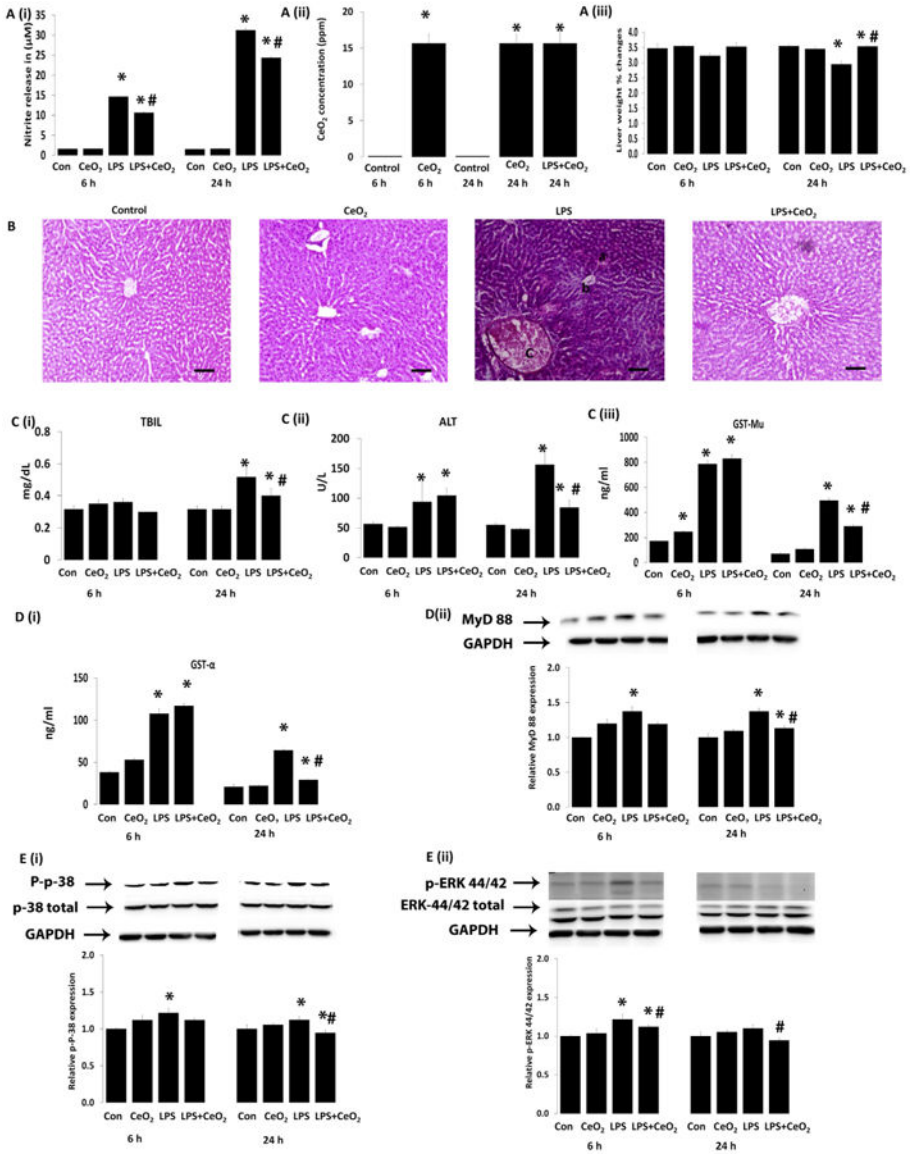

Fig. 3. Protective effect of CeO_2 nanoparticles on LPS-induced liver failure in vivo via MyD dependent MAP kinase pathway

A (i) nitric oxide production in serum, A (ii) presence of cerium in liver, A (iii) liver weight change. B histological change of liver (H & E, Scale bars = 100 μm), C (i) total bilirubin (TBIL), C (ii) alanine aminotransferase (ALT), C (iii) glutathione S transferae (GST-Mu) and D (i) glutathione S transferase (GST-α). Levels of total and phosphorylated proteins were determined by western blotting and normalized to GAPDH respectively, D (ii) MyD 88, E (i) P-p38, and E (ii) P-ERK 44/42. Samples were pooled from control (n = 6), CeO_2 (n = 6), Sepsis (n = 6), Sepsis + CeO_2 (n = 6) and analyzed in triplicate. Values are mean ± SEM of 3 independent experiments performed in triplicate. Statistical significance was determined by a one way ANOVA using Holm–Sidak test. $^{*}P < 0.05$ compared to control group, $^{*\#}P < 0.05$ compared to sepsis group.

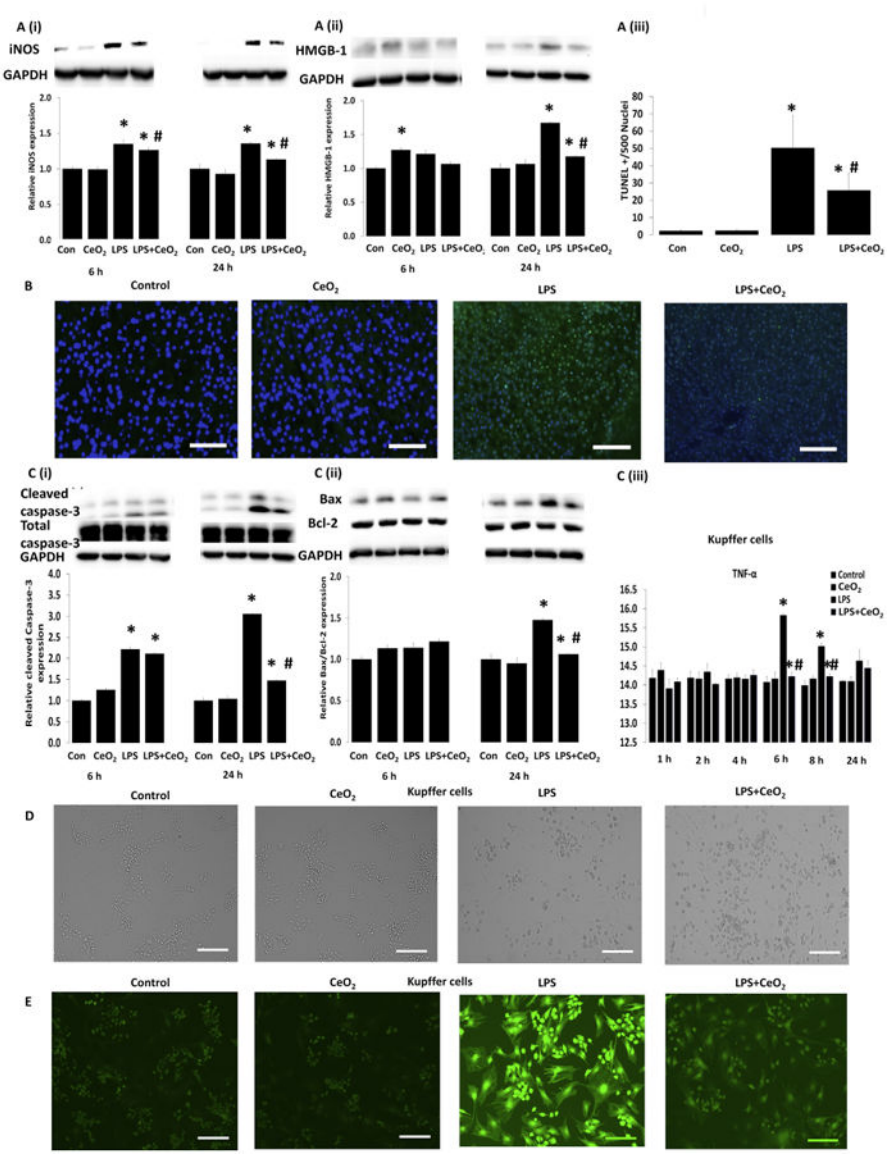

Fig. 4. Effect of CeO_2 nanoparticles on inflammatory mediators, apoptosis and Kupffer cell changes induced by LPS

Levels of inflammatory mediator proteins were determined by western blotting and normalized to GAPDH respectively: A (i) iNOS, A (ii) HMGB1. B mitochondria dependent apoptosis was determined by TUNEL staining (Scale bar = 100 μm), A (iii) quantification of TUNEL positive nuclei, C (i) total and cleaved caspase-3, and C (ii) Bax/Bcl-2 ratio. Samples were pooled from control (n = 6), CeO_2 (n = 6), Sepsis (n = 6), Sepsis + CeO_2 (n = 6) and analyzed in triplicate. Kupffer cell culture and changes: Cells were exposed to LPS in the presence and absence of CeO_2 nanoparticles for 24 h (D) morphological changes (Scale bar = 200 μm), C (iii) TNF-α, and (E) ROS production (Scale bar = 200 μm). Kupffer cells were isolated from three different animals from each group at 3 different time points (n = 3). Values are mean ± SEM of 3 independent experiments performed in triplicate. Statistical significance was determined by a one way ANOVA using Holm–Sidak test. $^{*}P < 0.05$ compared to control group, $^{*\#}P < 0.05$ compared to sepsis group.

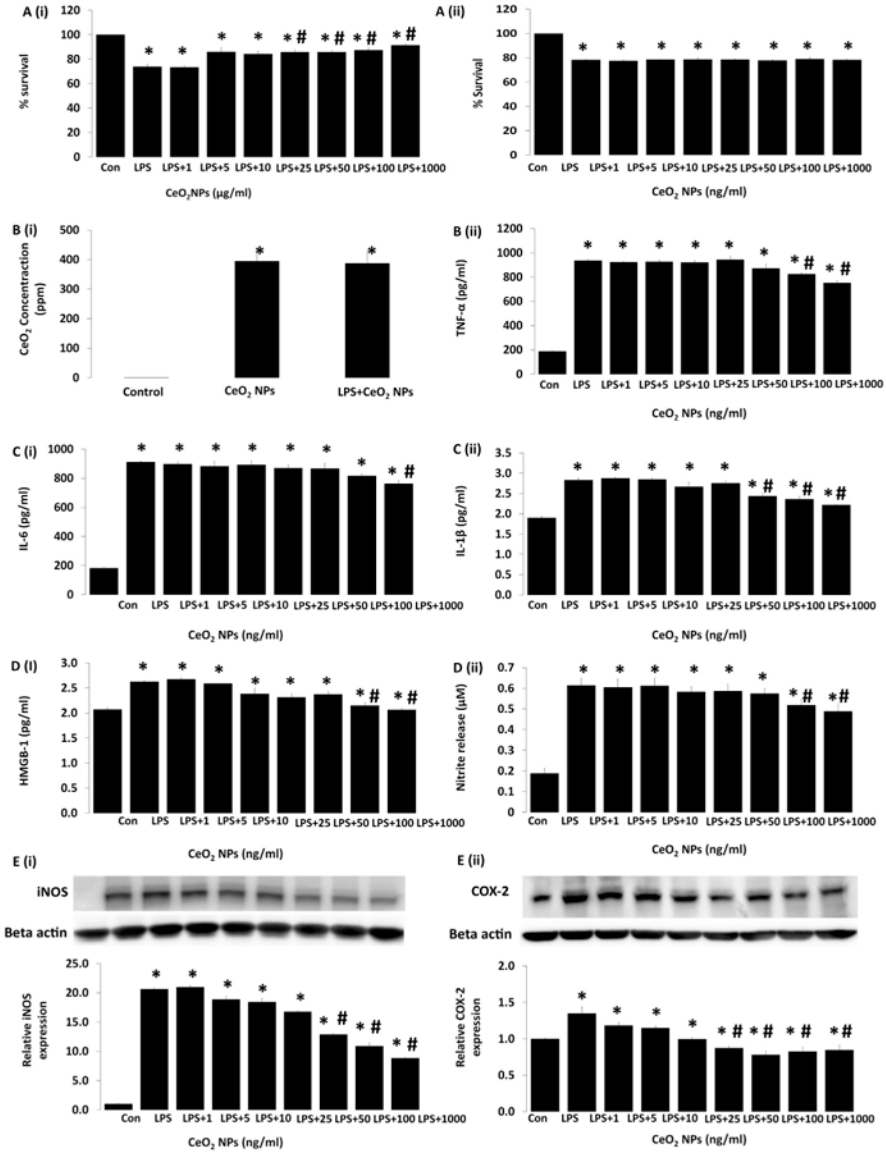

Fig. 5. Effect of CeO_2 nanoparticles on survival, ROS, Δψm, and cytokines production induced by LPS in RAW cells

Cells were exposed to LPS in the presence and absence of CeO_2 nanoparticles for 24 h. A (i) protective effect of CeO_2 nanoparticles against LPS insult, A (ii) CeO_2 nanoparticles does not have any tendency to bind with LPS and neutralizing the functionality of LPS. B (i) amount of cerium oxide uptake by macrophage confirmed by ICP-MS analysis, B (ii) tumor necrosis factor alpha (TNF-α). C (i) interleukin-6 (IL-6), C (ii) interleukin-1 beta (IL-1β). D (i) high mobility box group protein-1 (HMGB1), D (ii) measurement of nitrite in the medium as determined by ELISA and E (i) and E (ii) expression of iNOS and COX-2 by western blot analysis. Values are mean ± SEM of 3 independent experiments. Statistical significance was determined by a one way ANOVA using Holm–Sidak test. *Significant difference from control ($P < 0.05$). *# Significant difference from LPS treatment ($P < 0.05$).

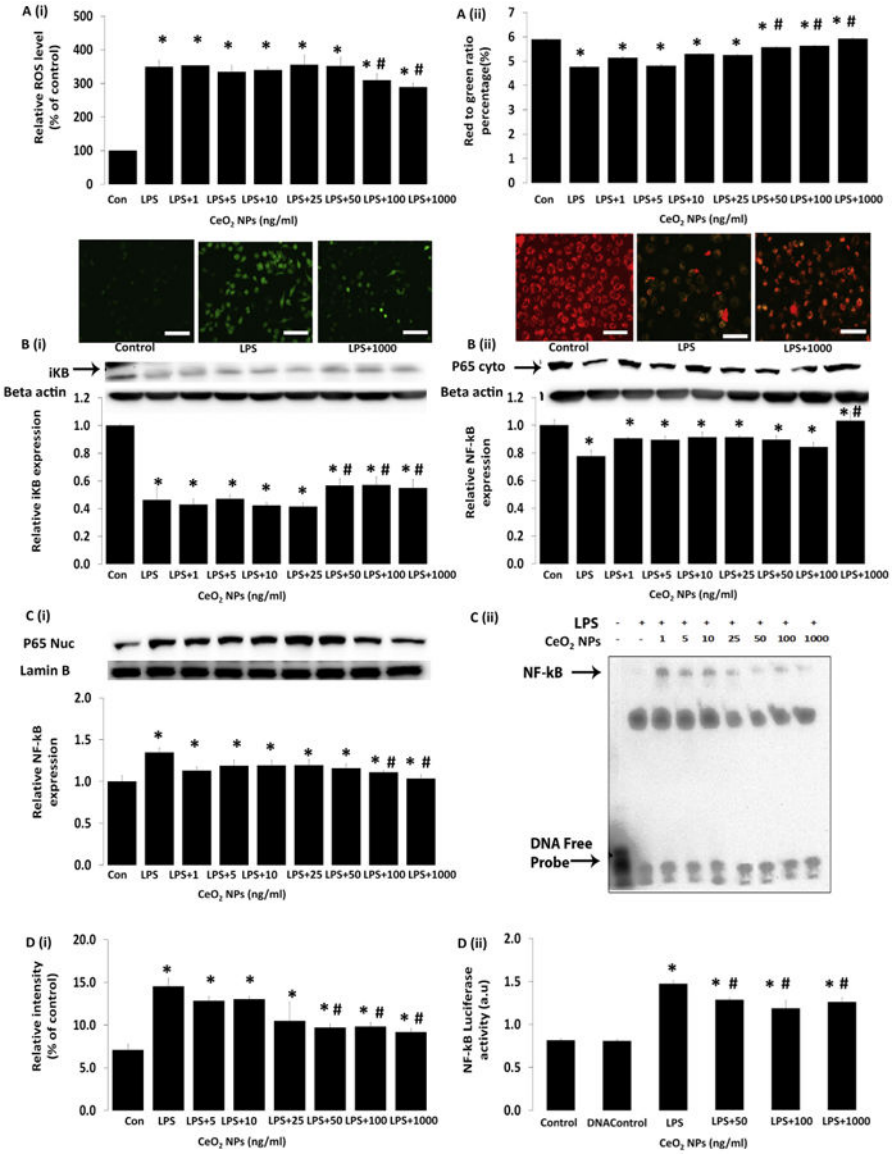

Fig. 6.

Effect of CeO_2 nanoparticles on NO production and the expression of iNOS and COX-2 and translocation of NF-kB/p65 in RAW 264.7 cells. Cells were exposed to LPS in the presence and absence of CeO_2 nanoparticles for 24 h. A (i) reactive oxygen species production (ROS) was determined by 2, 7-dichlorodihydrofluorescein diacetate (DCFH-DA) (Scale bar = 50 μm), A (ii) mitochondrial membrane potential (Δψm) was determined by JC-1 (Scale bar = 50 μm). B (i) expression of IkB-α in whole cell lysate, B (ii) measurement of NF-kB in cytoplasmic and nuclear extracts C (i) by immunoblotting, C (ii) a representative image of EMSA binding of NF-kB to DNA and quantification of EMSA by densitometry D (i), and D (ii) NF-kB luciferase activity by Luciferase reporter assay. Values are mean ± SEM of 3 independent experiments. *Significantly different from control ($P < 0.05$). *# Significantly different from LPS treatment ($P < 0.05$).